Solution Structure and Dynamics of Binuclear Dinitrogen Complexes of Bis(pentamethylcyclopentadienyl)titanium(II) and Bis(pentamethylcyclopentadienyl)zirconium(II)

Juan M. Manriquez, Donald R. McAlister, Edward Rosenberg, Alan M. Shiller, Kenneth L. Williamson, Sunney I. Chan,*[1] and John E. Bercaw*[1,2]

Contribution No. 5684 from the Arthur Amos Noyes Laboratory of Chemical Physics, California Institute of Technology, Pasadena, California 91125. *Received October 11, 1977*

Abstract: The solution structure and dynamics of $\{(\eta^5\text{-}C_5Me_5)_2ZrN_2\}_2N_2$, $\{(\eta^5\text{-}C_5Me_5)_2Zr(CO)\}_2N_2$, $\{(\eta^5\text{-}C_5Me_5)_2Zr(PF_3)\}_2N_2$, and $\{(\eta^5\text{-}C_5Me_5)_2TiN_2\}_2N_2$ have been studied by ^1H NMR spectrometry. $\{(\eta^5\text{-}C_5Me_5)_2ZrN_2\}_2N_2$ is observed to undergo mutual exchange of pentamethylcyclopentadienyl ligands between the two sites of the molecule on the time scale of the order of the ^1H NMR experiments at 10 °C. Variable-temperature ^{15}N NMR experiments for $\{(\eta^5\text{-}C_5Me_5)_2Zr(^{15}N_2)\}_2(^{15}N_2)$ were also carried out, and the results are interpreted on the basis of dissociative exchange of the two terminal dinitrogen ligands with free dissolved N_2. The observation that nitrogen dissociation is 5-10 times faster than $[\eta^5\text{-}C_5Me_5]$ site exchange suggests a mechanism for ring interchange involving stepwise dissociation-association of terminal N_2 ligands with "inversion" at the zirconium centers. Activation parameters calculated from ^{15}N NMR data are $E_a = 11$ kcal·mol^{-1} and $\Delta S^{\ddagger} = +10$ eu. The observed temperature dependence of the ^1H NMR spectra for the isostructural complex $\{(\eta^5\text{-}C_5Me_5)_2TiN_2\}_2N_2$ suggests that the same mechanism is operative. $\{(\eta^5\text{-}C_5Me_5)_2Zr(CO)\}_2N_2$, on the other hand, does not undergo CO dissociation at a rate sufficient to observe $[\eta^5\text{-}C_5Me_5]$ ring site exchange by ^1H NMR spectrometry even at 64 °C.

Bis(pentamethylcyclopentadienyl) derivatives of titanium and zirconium have proved to be useful congeners to their bis(cyclopentadienyl) analogues by virtue of enhanced stability, solubility, and crystallizability. Dinitrogen complexes of $(\eta^5\text{-}C_5Me_5)_2Ti$ and $(\eta^5\text{-}C_5Me_5)_2Zr$ are of particular interest in view of the ready protonation and reduction to hydrazine of their ligated N_2.[3-8] We have recently reported the solid-state structures of $\{(\eta^5\text{-}C_5Me_5)_2Ti\}_2N_2$[8] and $\{(\eta^5\text{-}C_5Me_5)_2ZrN_2\}_2N_2$[7] as determined by single-crystal x-ray diffraction methods. In this paper we report the results of an NMR and IR study of the solution structure and dynamics of $\{(\eta^5\text{-}C_5Me_5)_2ZrN_2\}_2N_2$, its carbonyl and PF_3 derivatives, and the titanium analogue.

Experimental Section

Physical Measurements. ^1H NMR spectra were recorded on a Varian HR 220 (CW) spectrometer. ^{15}N NMR spectra were obtained at 18.25 MHz on a Bruker WH180 (FT) spectrometer. Computer-synthesized spectra were obtained using DNMR3, a general NMR line-shape program with symmetry and magnetic equivalence factoring, written by Binsch and Kleier.[9] Infrared spectra were obtained on Perkin-Elmer 180, 225, and 457 and Beckman IR-12 spectrophotometers.

Materials. All manipulations were performed on a vacuum line, in a glovebox which was evacuated to <0.05 Torr and filled just prior to use with either prepurified argon or nitrogen, or in a Vacuum Atmospheres glovebox under nitrogen. Nitrogen used in the experiments was prepurified grade rendered rigorously oxygen- and water-free by passage over MnO on vermiculite[10] and activated 4A molecules sieves. Toluene, benzene, and 30-60 °C petroleum ether were purified by vacuum transfer first from $LiAlH_4$ and then from "titanocene".[11] 1,2,3,4,5-Pentamethylcyclopentadiene and $\{(\eta^5\text{-}C_5Me_5)_2Ti\}_2N_2$ were prepared as described earlier.[11] $^{15}N{\equiv}^{14}N$ was prepared in aqueous solution from $(^{15}NH_4)_2SO_4$ (Merck Sharpe and Dohme) and $NaNO_2$; nitric oxide was removed with $FeSO_4$, then $^{15}N{\equiv}^{14}N$ was collected via a Toepler pump. Both $^{15}N{\equiv}^{15}N$ and $^{15}N{\equiv}^{14}N$ were rendered rigorously water- and oxygen-free by contact with solid $\{C_5(CH_3)_5\}\{C_5(CH_3)_4CH_2\}Ti$,[4] and finally examined by mass spectrometry.[12]

Procedures. 1. $(\eta^5\text{-}C_5Me_5)_2ZrCl_2$. 1,2-Dimethoxyethane (300 mL) was vacuum transferred from $LiAlH_4$ to a 500-mL three-neck flask. $C_5(CH_3)_5H$ (20.4 g, 150 mmol), then 70 mL (150 mmol) of *n*-butyllithium were added at −80 °C via syringe. This mixture was warmed slowly to room temperature and stirred for 30 min. The mixture was cooled again to −80 °C, and 15.3 g (63 mmol) of freshly sublimed $ZrCl_4$ was added. This mixture was warmed to 25 °C, then heated at reflux for 3 days. Solvent was removed under reduced pressure to leave a thick, pale brown residue, which was taken up in 250 mL of $CHCl_3$ and 100 mL of 6 M HCl. The aqueous layer was separated and washed with $CHCl_3$. The combined chloroform layers were washed once with distilled water, dried over Na_2SO_4, then concentrated to approximately 50 mL. Petroleum ether (200 mL, 90-100 °C) was added and solvent slowly removed by rotary evaporation. The residual solution (~50 mL) was cooled, and the product was filtered off and washed with cold petroleum ether, yield 15 g of pale yellow crystals (55%). Anal. Calcd for $C_{20}H_{30}Cl_2Zr$: C, 55.56; H, 6.94; Cl, 16.40; Zr, 21.10. Found: C, 55.57; H, 6.99; Cl, 16.36; Zr, 21.21. NMR (chloroform-d_1): s, δ 2.00.

2. $\{(\eta^5\text{-}C_5Me_5)_2ZrN_2\}_2N_2$. To 5.0 g of $(\eta^5\text{-}C_5Me_5)_2ZrCl_2$, 20 mL of Hg, and 80 mL of benzene was added 2.5 mL of 40 wt % Na/Hg (2.5 g Na) under N_2 with stirring and cooling. This mixture was stirred vigorously at room temperature for 3 days under 1 atm N_2. The resultant dark red solution was decanted from the bulk of the amalgam and filtered. The amalgam was washed with 20 mL of fresh benzene, which was also filtered. The combined filtrates were reduced in volume as quickly as possible to approximately 10 mL, 40 mL of 30-60 °C petroleum ether added, and the resulting solution allowed to stand under N_2 for 20 h. The product was then filtered off, washed three times at low temperature with 10-mL portions of 30-60 °C petroleum ether, dried in vacuo, and finally transferred to a storage ampule in a nitrogen-filled glovebox, yield 2.36 g of metallic green crystals (51%). Anal. Calcd for $C_{40}H_{60}N_6Zr_2$: C, 59.54; H, 7.44; N, 10.41; Zr, 22.61. Found: C, 59.75; H, 7.36; N, 10.18; Zr, 22.77.

3. $\{(\eta^5\text{-}C_5Me_5)_2ZrN_2\}_2N_2$ Labeled with $^{15}N{\equiv}^{15}N$ or $^{15}N{\equiv}^{14}N$. Toluene and N_2 were slowly removed from a solution of $\{(\eta^5\text{-}C_5Me_5)_2ZrN_2\}_2N_2$ over a 3-h period at room temperature, yielding a red-orange, crystalline mass of $\{C_5(CH_3)_5\}\{C_5(CH_3)_4CH_2\}ZrH$.[8] This complex was dissolved in 15 mL of 30-60 °C petroleum ether, a small amount of yellow precipitate filtered off, and either $^{15}N{\equiv}^{15}N$ or $^{15}N{\equiv}^{14}N$ admitted. After 20 h the product was filtered, washed, and dried as before. ^{15}N NMR samples were prepared in toluene-d_8, filtered into 10-mm diameter NMR tubes, and sealed under approximately 1 atm of $^{15}N{\equiv}^{15}N$ or $^{15}N{\equiv}^{14}N$.

4. $\{(\eta^5\text{-}C_5Me_5)_2Zr(CO)\}_2N_2$. To 139 mg (0.172 mmol) of $\{(\eta^5\text{-}C_5Me_5)_2ZrN_2\}_2N_2$ were added 8 mL of toluene and 1.060 mmol of CO at liquid nitrogen temperature. The mixture was warmed to −23 °C and stirred vigorously for 1 h. After the dark red solution was cooled to −80 °C the residual gas mixture (1.025 mmol) was collected by means of a Toepler pump. CO was oxidized to CO_2 by circulation through CuO at 320 °C and trapped at liquid nitrogen temperature. Residual N_2 (0.337 mmol, 1.95 mmol N_2/mmol Zr) was collected and discarded, then CO_2 was collected from the trap at −80 °C (corresponding to 0.683 mmol of residual CO). The amount of CO absorbed was thus 0.377 mmol (2.18 mmol CO/mmol Zr). In a separate experiment 674 mg of $\{(\eta^5\text{-}C_5Me_5)_2ZrN_2\}_2N_2$ in toluene was

0002-7863/78/1500-3078$01.00/0

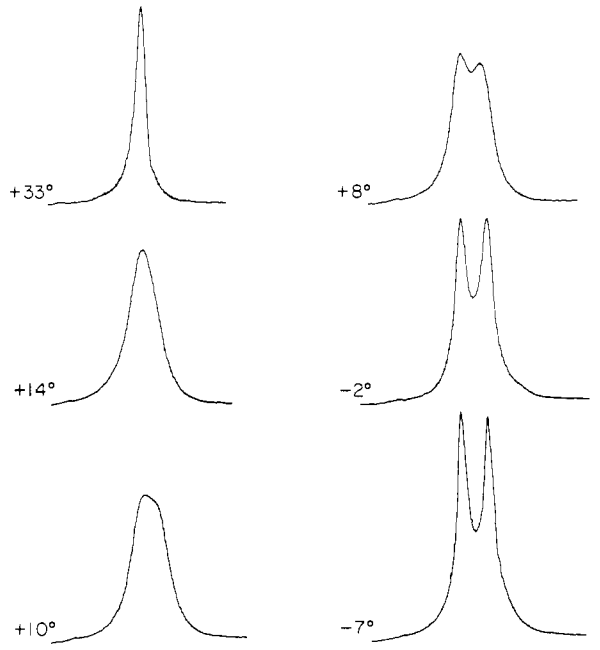

Figure 1. ^{1}H NMR spectra for $\{(\eta^5\text{-}C_5Me_5)_2ZrN_2\}_2N_2$ in toluene-d_8.

treated with excess CO at −23 °C for 1 h. Toluene was then removed slowly in vacuo at −20 °C, petroleum ether added, and the resulting green crystalline product filtered, washed, and dried as before. Anal. Calcd for $C_{42}H_{60}N_2O_2Zr_2$: C, 62.48; H, 7.49; N, 3.47. Found: C, 59.88; H, 7.25; N, 3.24.

5. $\{(\eta^5\text{-}C_5Me_5)_2Zr(PF_3)\}_2N_2$. To 112 mg (0.139 mmol) of $\{(\eta^5\text{-}C_5Me_5)_2ZrN_2\}_2N_2$ were added 8 mL of toluene and 0.536 mmol of PF_3 at −80 °C. The mixture was warmed to −23 °C and stirred for 15 min at this temperature. After the solution was cooled back to −80 °C, N_2 (0.257 mmol, 1.86 mmol/mmol Zr) was collected through a series of three liquid nitrogen cooled traps, then discarded. The traps were warmed to −80 °C and residual PF_3 (0.272 mmol) was collected. The amount of PF_3 absorbed was thus 0.264 mmol (1.90 mmol/mmol Zr). $\{(\eta^5\text{-}C_5Me_5)_2Zr(PF_3)\}_2N_2$ was isolated using the procedure for $\{(\eta^5\text{-}C_5Me_5)_2Zr(CO)\}_2N_2$.

Results

^{1}H NMR spectra of $\{(\eta^5\text{-}C_5Me_5)_2ZrN_2\}_2N_2$ (**1**) in toluene-d_8 at various temperatures are shown in Figure 1, and the results are summarized in Table I. The spectrum at −26 °C is readily interpreted on the basis of the structure determined by x-ray diffraction methods (structure **1**). Thus the two singlets are attributed to the pairwise equivalent $[\eta^5\text{-}C_5(CH_3)_5]$ rings, although the difference in their chemical shifts is quite small, amounting to only 3.4 Hz at 220 MHz at this temperature. In the range −26 to 50 °C the two signals steadily broaden, coalesce at approximately 11 °C, and finally give rise to a single line which narrows to a limiting width at half-height of 1.9 Hz at 50 °C.

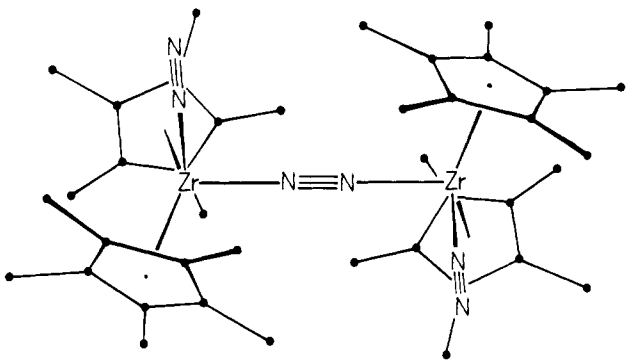

1

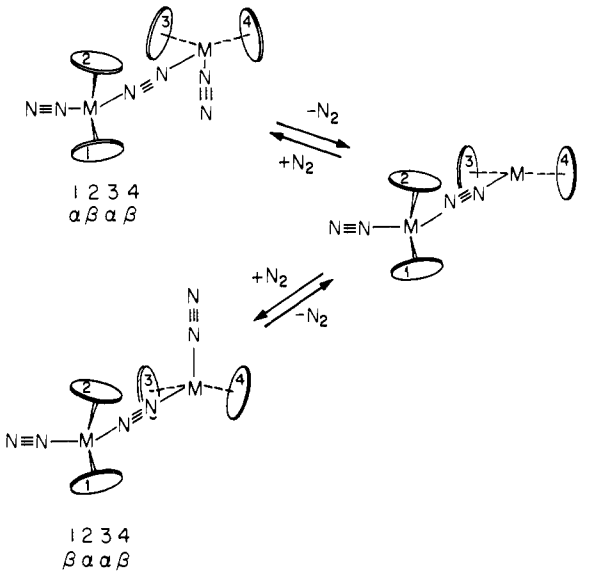

Figure 2. Rearrangement for **1** which interchanges $(\eta^5\text{-}C_5Me_5)$ rings 1 and 2 between the two types of sites (α and β).

Table I. Summary of ^{1}H NMR Data for $\{(\eta^5\text{-}C_5Me_5)_2ZrN_2\}_2N_2$ (Toluene-d_8)

Temp, °C	δ_1 (line width, Hz)	δ_2 (line width, Hz)
−26	1.77 (2.4)	1.79 (3.0)
−20	1.77 (2.4)	1.79 (2.7)
−7	1.77 (2.7)	1.79 (2.7)
−2	1.77 (3.0)	1.79 (2.8)
4	1.79	1.80
8	1.80	
11	1.80 (6.8)	
14	1.80 (5.8)	
20	1.80 (4.0)	
33	1.80 (2.2)	
50	1.80 (1.9)	

A reasonable interpretation of these spectral observations is that the two types of $[\eta^5\text{-}C_5(CH_3)_5]$ rings undergo mutual site exchange on the time scale of the order of these NMR experiments. A possible mechanism for simultaneous interchange of the two ring environments would involve simple 180° rotation about one (or both) of the Zr-μ-N_2 bonds of the dimer via either a cis or trans intermediate.

If this were the case, the proton spectra could be simulated on the basis of a two-site exchange. To show this, let (1,2) and (3,4) denote the cyclopentadienyl rings attached to the two zirconiums (see Figure 2). In the solid state structure the magnetic environments of rings 1 and 3 are identical, as are rings 2 and 4. If we denote these environments by α (for a cyclopentadienyl ring eclipsed with a terminal dinitrogen ligand) and β, respectively, then the effect of a twofold rotation about the Zr-μ-N_2 bond can be represented by

$$(1\alpha,2\beta)(3\alpha,4\beta) \xrightarrow[\text{rotation}]{180°} (1\beta,2\alpha)(3\beta,4\alpha)$$

The ^{1}H NMR spectrum can be fitted to such a model. The rate constants which we obtained for this exchange process caused by this twofold rotation are summarized as a function of temperature in Table II.

The above analysis, of course, assumes that the terminal dinitrogen ligands do not undergo dissociation from zirconium at rates comparable to the twofold rotation proposed above. Two important features emerge if the terminal dinitrogens can undergo dissociation. First, dissociation of a terminal dini-

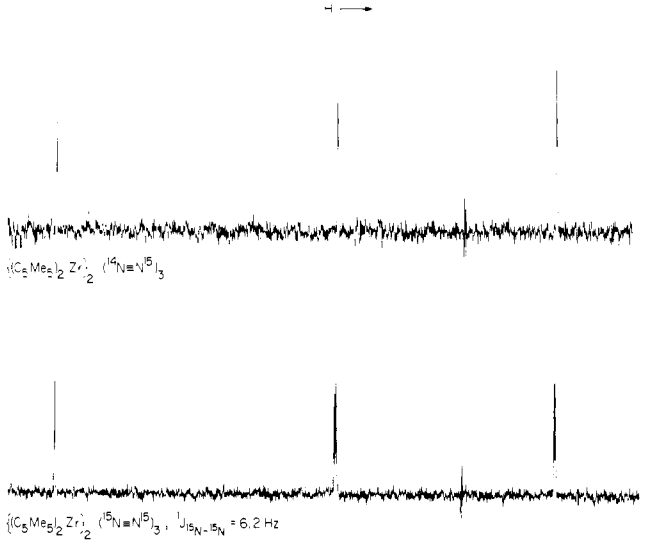

Figure 3. 18.25-MHz ^{15}N NMR spectra for **1**-($^{15}N_2$)$_3$ and **1**-($^{15}N{\equiv}^{14}N$)$_3$ in toluene-d_8 at −28 °C.

Table II. Rate Constants from the Best Fit of ^1H NMR Spectra to Two-Site and Four-Site Exchange Mechanisms for $\{(\eta^5\text{-}C_5Me_5)_2ZrN_2\}_2N_2$.

Temp, °C	k, s^{-1}	
	2-site model	4-site model
42.5	23.0	12.6
31	15.5	8.0
19	10.3	5.1
15	9.0	4.5
10	6.5	3.1
5	6.3	3.0
1	4.5	2.2

trogen from one zirconium can lead to exchange of the magnetic environments of the cyclopentadienyl rings at the other zirconium provided that the reverse reaction can lead to a change in configuration ("inversion") at the zirconium to which the nitrogen molecule returns. This process can best be seen by examining Figure 2. Secondly, such a dissociation process should lead to averaging of the magnetic environments of the N atoms of such a terminal dinitrogen ligand if the rate is sufficiently rapid. If the rate is not too slow compared with the chemical shift difference between distal and proximal nitrogens, one might at least expect broadening of the signals due to these nitrogens. In view of the latter possibility ^{15}N NMR experiments were undertaken.

The 18.25-MHz ^{15}N NMR spectrum for **1**-($^{15}N_2$)$_3$ in toluene-d_8 at −28 °C is given in Figure 3. The spectrum is readily interpreted on the basis of the solid-state structure. The singlet 185 ppm downfield of HNO_3 is attributed to the two equivalent ^{15}N nuclei of the μ-N_2 and the two doublets centered 86 and 17 ppm downfield of HNO_3 to the proximal and distal nitrogen atoms of the two equivalent terminal dinitrogen ligands ($^1J_{^{15}N\text{-}^{15}N}$ = 6.2 Hz). The ^{15}N NMR spectrum of **1**-($^{15}N{\equiv}^{14}N$)$_3$ (Figure 3) exhibits the same spectrum except that the two upfield doublets now appear as the expected singlets.

On the basis of the rotation mechanism no temperature dependence of the ^{15}N NMR spectrum for **1** is predicted, except for bulk susceptibility effects and possible differential shifts due to solvent interactions. As can be seen in Figures 3 and 4, however, on warming **1**-($^{15}N_2$)$_3$ from −28 to 50 °C, the signals due to the two terminal dinitrogen ligands steadily broaden. In contrast, the singlet attributable to the μ-N_2 remains sharp over the entire temperature range. Mutual site

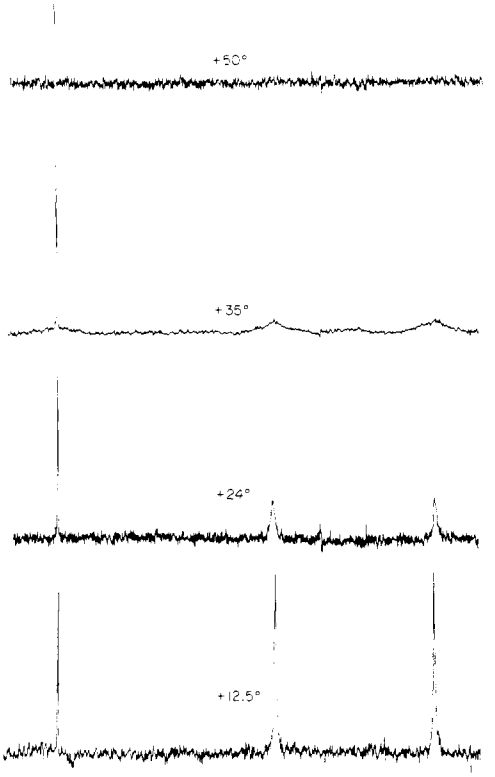

Figure 4. Variable temperature ^{15}N NMR spectra for **1**-($^{15}N_2$)$_3$.

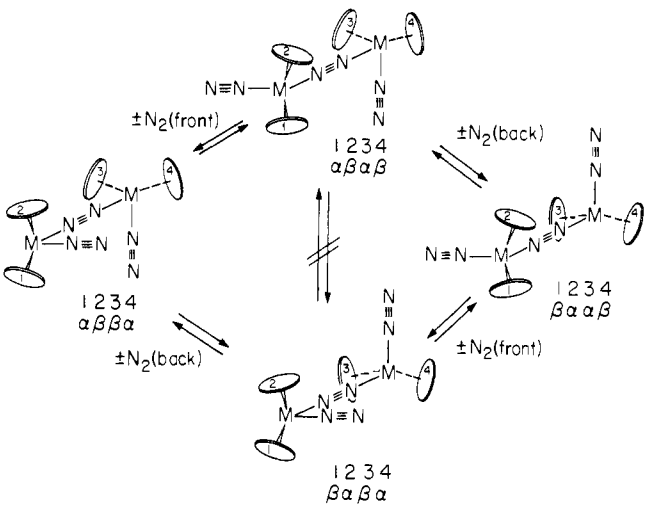

Figure 5. Sequence which interchanges all four (η^5-C_5Me_5) rings of **1**.

exchange of the two nitrogen nuclei of the two terminal dinitrogen ligands between the proximal and distal positions relative to zirconium could account for the observed temperature dependence of the ^{15}N NMR spectra. Significantly, the rate of this process, estimated from line width data, is comparable to the rate of [η^5-$C_5(CH_3)_5$] ring site exchange. In fact, the rate of proximal–distal nitrogen interconversion deduced according to a two-site mutual site exchange calculation is faster than the rate of [η^5-$C_5(CH_3)_5$] ring site exchange by a factor of 5–10. It therefore appears that dissociation of the terminal dinitrogen ligands can also contribute to the [η^5-$C_5(CH_3)_5$] site exchange.

We now consider this mechanism in greater detail. The effect of dissociation of dinitrogen ligands on the ^1H and ^{15}N NMR spectra can be ascertained by considering the mechanism depicted by Figures 2 and 5. The first step (Figure 2)

Table III. Kinetic Parameters for Best Fit of ^{15}N NMR Spectra (Three-Site Model)

Temp, °C	$k(^{15}N)$, s^{-1}
−28	
12.5	43
24	95

involves dissociation of one of the terminal dinitrogen ligands of **1**. The resulting intermediate may be expected to rearrange, assuming a planar trigonal arrangement of $[\eta^5\text{-}C_5(CH_3)_5]$ ring centroids and the μ-N_2 at the coordinatively unsaturated zirconium center, a local ligand geometry about Zr entirely analogous to that established for titanium for $\{(\eta^5\text{-}C_5Me_5)_2Ti\}_2N_2$.[8] **1** is regenerated by addition of N_2 to either side of the coordinatively unsaturated zirconium center. This reverse reaction should have no effect on the magnetic environments of the cyclopentadienyl rings if it occurs with retention of configuration at the zirconium center.

We note, however, that "inversion" at one zirconium center for **1** effects $[\eta^5\text{-}C_5(CH_3)_5]$ ring exchange between the two environments α,β only at the other Zr. Thus at least two such sequences involving each of the two terminal dinitrogen ligands are required to effect complete site exchange for all four $[\eta^5\text{-}C_5(CH_3)_5]$ rings. This point is illustrated in Figure 5. If we write the kinetic steps as

$$\begin{array}{ccc} (1\alpha, 2\beta)(3\alpha, 4\beta) & \underset{k}{\overset{k}{\rightleftharpoons}} & (1\beta, 2\alpha)(3\alpha, 4\beta) \\ k \Updownarrow k & & k \Updownarrow k \\ (1\alpha, 2\beta)(3\beta, 4\alpha) & \underset{k}{\overset{k}{\rightleftharpoons}} & (1\beta, 2\alpha)(3\beta, 4\alpha) \end{array}$$

the computer simulation of the ^1H NMR data based on this exchange model leads to the rate constants summarized in Table II. A comparison of the rate constants deduced from the two-site (rotation) and four-site (N_2 dissociation) exchange models shows that the rate constants in the case of the four-site exchange model are ~50% that of the two-site model at the same temperature, as expected.

It is important to note that in the above analysis we have not made the assumption that the addition of nitrogen (N_2) to the coordinatively unsaturated zirconium center for the intermediate $(\eta^5\text{-}C_5Me_5)_2(N_2)Zr\text{-}N_2\text{-}Zr(C_5Me_5)_2$ occurs equally for either side. If this is the case, then the rate of nitrogen dissociation is expected to be four times faster than the rate of site exchange for all four $[\eta^5\text{-}C_5(CH_3)_5]$ rings. This ratio is clearly a lower limit. A comparison of the rate of site exchange for the ring protons from the ^1H NMR data with the rate of N_2 dissociation determined by the ^{15}N NMR data would be revealing.

Analysis of the ^{15}N NMR data is unfortunately quite complex. First of all, N_2 dissociation would contribute toward averaging of the ^{15}N chemical shift for the proximal and distal positions of the terminal N_2 ligands due to proximal–distal interconversion. Secondly, there exists the possibility of equilibration with free N_2 in solution. Under the conditions of our ^{15}N experiments, where [**1**] ≅ 50 mM, the free N_2 concentration in equilibrium with the complex in solution was estimated to be ~5 mM. In an independent experiment, the chemical shift of the free dinitrogen in toluene-d_8 was measured to be 65.5 ppm upfield of nitric acid ($H^{15}NO_3$). Fortunately, the rate of N_2 dissociation is slow compared with the chemical shift difference between the bound and free forms, as well as that between the distal and proximal positions of the terminal nitrogen ligands. Since the N_2 dissociation is relatively slow compared to the NMR time scale of observation in these

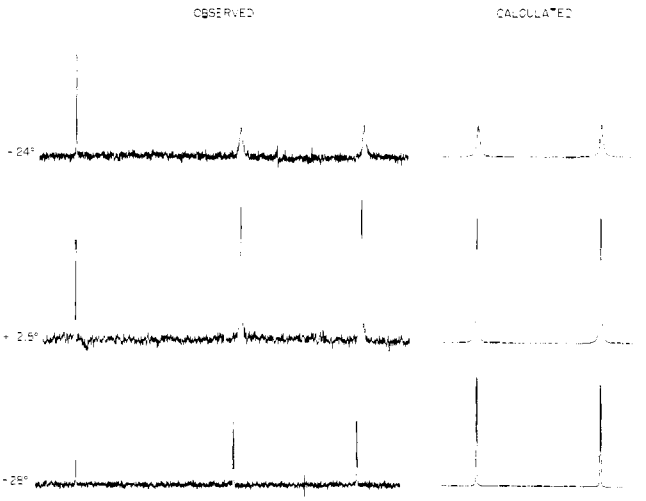

Figure 6. Observed and calculated ^{15}N NMR spectra for **1**-$(^{15}N_2)_3$.

experiments, the kinetic parameters deduced from the line shape are not too sensitive to the detailed model used to describe the dissociation process. Computer-synthesized ^{15}N spectra based upon the mechanism

$$\underset{\gamma\ \ \delta}{N\equiv N} \underset{k'}{\overset{k}{\rightleftharpoons}} \underset{\epsilon\ \ \epsilon}{N\equiv N} \underset{k}{\overset{k'}{\rightleftharpoons}} \underset{\delta\ \ \gamma}{N\equiv N}$$

(free)

are depicted in Figure 6 and the kinetic parameters needed to best fit the observed spectra at the various temperatures are summarized in Table III. A comparison of these data with the kinetic parameters deduced from the ^1H NMR data indicate that $k(^{15}N)/k(^1H) \sim 10$, in fair agreement with the predicted statistical ratio.

^1H NMR spectra for **1** under 0.5 atm of N_2 or for samples prepared under argon showed no significant difference from those measured under 1 atm of N_2; in particular, coalescence occurs at the same temperature. This result suggests that the rate-determining step in the mechanism is dissociation of a terminal dinitrogen ligand from **1**. The activation parameters E_a = 11 kcal mol^{-1}, $\Delta S^{\ddagger}$ = +10 eu calculated from ^{15}N NMR data are reasonable for such a unimolecular step.

The lability of the terminal dinitrogen ligands of **1** has been further substantiated by N_2 substitution experiments carried out with **1**-$(^{15}N_2)_3$.[6] When this complex was treated with natural $^{14}N_2$ in toluene complete exchange of only two of the three dinitrogen ligands was found at −23 °C after 15 min. This observation requires that under these conditions exchange occurs between free N_2 and only the two equivalent terminal dinitrogen ligands of **1**.

Treatment of **1** with CO or PF_3 yields $\{(\eta^5\text{-}C_5Me_5)_2Zr(CO)\}_2N_2$ (**2**) and $\{(\eta^5\text{-}C_5Me_5)_2Zr(PF_3)\}_2N_2$ (**3**), respectively (eq 1 and 2), which may be isolated as metallic green crystalline materials. On the basis of their characteristic color, their IR spectra (Table IV), and ^1H NMR spectra (see below), **2** and **3** appear to have structures identical with **1** with CO and PF_3 substituted for the terminal dinitrogen ligands. **2** exhibits a ^1H NMR spectrum (toluene-d_8) consisting of two singlets of equal intensity at 1.80 and 1.82 ppm at −48 °C. Except for small chemical shift variations, this spectrum is maintained up to 64 °C (further heating results in sample decomposition). $[\eta^5\text{-}C_5(CH_3)_5]$ ring exchange for **2** is thus much slower than for **1**, indicating lower lability for the terminal carbonyls.

$$\underset{\mathbf{1}}{\{(\eta^5\text{-}C_5Me_5)_2ZrN_2\}_2N_2} + 2CO \xrightarrow{-23\ ^\circ C} \underset{\mathbf{2}}{\{(\eta^5\text{-}C_5Me_5)_2Zr(CO)\}_2N_2} + 2N_2 \quad (1)$$

Table IV. Infrared Data

	Sample form	ν(NN), cm^{-1}	ν(CO), cm^{-1}
$\{(\eta^5\text{-}C_5Me_5)_2\text{-}ZrN_2\}_2N_2$	KBr pellet	2040 (m) 2003 (s) 1578 (m)	
	Nujol mull	2041 (m) 2006 (s) 1556 (m)	
	Pentane solution	2047 (m) 2014 (s) *a*	
$\{(\eta^5\text{-}C_5Me_5)_2\text{-}Zr(^{14}N^{15}N)\}_2\text{-}(^{14}N^{15}N)$	Nujol mull	2006 (m) 1970 (s) 1530 (m)	
$\{(\eta^5\text{-}C_5Me_5)_2\text{-}Zr^{15}N_2\}_2{}^{15}N_2$	Nujol mull	1972 (m) 1937 (s) 1515 (m)	
	Toluene-d_8 solution	1975 (s) 1937 (vs) *a*	
$\{(\eta^5\text{-}C_5Me_5)_2\text{-}Zr(CO)\}_2N_2$	Nujol mull	1682 (m)	1902 (m) 1860 (s)
$\{(\eta^5\text{-}C_5Me_5)_2\text{-}Zr(PF_3)\}_2N_2$	Nujol mull	1655 (vw)	
$\{(\eta^5\text{-}C_5Me_5)_2\text{-}TiN_2\}_2N_2$	Nujol mull	2058 (m) 2020 (s) 1711 (m)	
	Heptane solution	2056 (m) 2023 (s) *a*	

[a] Cut off below ~1800 cm^{-1} owing to cell window (sapphire) and solvent absorptions.

$$\underset{\mathbf{1}}{\{(\eta^5\text{-}C_5Me_5)_2ZrN_2\}_2N_2} + 2PF_3 \xrightarrow{-23\ ^\circ C} \underset{\mathbf{3}}{\{(\eta^5\text{-}C_5Me_5)_2Zr(PF_3)\}_2N_2} + 2N_2 \quad (2)$$

Unlike **1** and **2**, **3** exhibits low stability in solution, decomposing over a period of several minutes at room temperature, thus precluding an accurate NMR study. However, at −76 °C the ^{1}H NMR spectrum of **3** (toluene-d_8) exhibits the expected two singlets of equal intensity at 1.79 and 1.81 ppm. These two signals coalesce at approximately −35 °C and give rise to a single line which narrows steadily to −6 °C where decomposition sets in. While this behavior could be taken to indicate a higher lability of PF_3 relative to N_2, this is difficult to reconcile considering the ability of PF_3 to quantitatively displace the two terminal dinitrogen ligands of **1**. In view of this unexpected behavior and the fact that the decomposition mechanism and product(s) for **3** are as yet undefined, we hesitate to interpret these NMR data in terms of a specific reversible, dynamic process.

The definition of the solution structure and dynamics for **1** serves to clarify the structure of its titanium analogue, $\{(\eta^5\text{-}C_5Me_5)_2TiN_2\}_2N_2$ (**4**), which was originally (and incorrectly) assigned the formula $(\eta^5\text{-}C_5Me_5)_2TiN_2$.[3,4,8] On the basis of its infared spectrum (Table IV) and its ^{1}H NMR and ^{15}N NMR spectra, there can be little doubt that the structure of **4** is entirely analogous to that for **1**. The ^{1}H NMR spectrum for **4** (toluene-d_8) exhibits two singlets of equal intensity at 1.55 and 1.63 ppm at −78 °C, which coalesce at approximately −42 °C. At higher temperatures this signal loses intensity and further broadens due to the onset of dissociative exchange with the two paramagnetic species $\{(\eta^5\text{-}C_5Me_5)_2Ti\}_2N_2$ and $(\eta^5\text{-}C_5Me_5)_2Ti$ (eq 3). In view of these complications no attempt

$$2(\eta^5\text{-}C_5Me_5)_2Ti \overset{N_2}{\rightleftharpoons} \{(\eta^5\text{-}C_5Me_5)_2Ti\}_2N_2 \overset{2N_2}{\rightleftharpoons} \{(\eta^5\text{-}C_5Me_5)_2TiN_2\}_2N_2 \quad (3)$$

was made to analyze these ^{1}H NMR data for **4** using the model shown in Figures 2 and 5. The high lability of the dinitrogen ligands for **4** and its ^{1}H NMR spectra over the temperature region −78 to −42 °C are, however, in full accord with this mechanism for $[\eta^5\text{-}C_5(CH_3)_5]$ ring site exchange.

Discussion

These studies implicate a fluxional behavior for complexes of the type $\{(\eta^5\text{-}C_5Me_5)_2MN_2\}_2N_2$ (M = Ti, Zr) involving $[\eta^5\text{-}C_5(CH_3)_5]$ site exchange coupled with terminal N_2 dissociation. While we cannot rule out the possibility that rotation about one (or both) of the μ-N_2 bonds also occurs in solution, we can state that it must be much slower. Indeed the barrier to rotation for $\{(\eta^5\text{-}C_5Me_5)_2Zr(CO)\}_2N_2$ must be greater than ~10 kcal mol^{-1}, since no ring site exchange (by either mechanism) is observable by ^{1}H NMR even at 64 °C. A greater barrier to rotation is expected for $\{(\eta^5\text{-}C_5Me_5)_2ZrN_2\}_2N_2$ as judged by the lower NN stretching frequency for its μ-N_2. Although steric crowding of $[\eta^5\text{-}C_5(CH_3)_5]$ rings may make some contribution, this high barrier is also attributable to considerable π character in the Zr–N_2–Zr bonding. This situation whereby **1** is locked firmly in the gauche configuration is entirely consistent with the qualitative MO picture presented earlier.[7]

The lability of the terminal dinitrogen ligands of **1** inferred from ^{1}H and ^{15}N NMR data has been demonstrated by exchange experiments carried out at −23 °C with $^{14}N_2$ and **1**-$(^{15}N_2)_3$. Exchange of the two terminal N_2 ligands of **1** with gaseous N_2 was found to proceed with an apparent rate constant of 4.5 (2) × 10^{-3} s^{-1}. By applying the Basolo and Wojcicki modification[14] of the McKay equation[15] for isotopic exchange, a true rate constant of 2.8 (5) s^{-1} is obtained for exchange of the terminal dinitrogen ligands with dissolved N_2. This value is in fair agreement with the value (0.67 s^{-1}) predicted by extrapolation of the ^{1}H and ^{15}N NMR kinetic data to −23 °C.

We recently reported the results of a labeling study of the reaction of **1** with HCl using $\{(\eta^5\text{-}C_5Me_5)_2Zr(^{14}N_2)\}_2(^{15}N_2)$, designed to establish which dinitrogen is reduced to hydrazine. The NMR study reported here demonstrates that this complex retains its integrity, since no exchange of terminal and bridging dinitrogen ligands is observed by ^{15}N NMR, even at 50 °C. An extrapolation of our data to −95 °C, the temperature maintained during the reaction of **1** with HCl, gives an estimated half-life for terminal dinitrogen dissociation of 3000 s, much greater than the visually estimated half-life (5 s) of the reaction of **1** with a 20 M excess of HCl at −95 °C. This result appears to preclude the possibility that the symmetric intermediate (e.g., $(\eta^5\text{-}C_5Me_5)_2Zr(N_2H)_2$) is generated by addition of HCl across the Zr-μ-N_2 bond of the coordinatively unsaturated zirconium center of $(\eta^5\text{-}C_5Me_5)_2(N_2)Zr\text{–}N_2\text{–}Zr(\eta^5\text{-}C_5Me_5)_2$. These results are not, however, inconsistent with the scheme postulated earlier:[6] protonation of a terminal N_2 of **1** followed by loss of the other terminal N_2 to generate $(\eta^5\text{-}C_5Me_5)_2Zr(N_2H)_2$.

Acknowledgments. This work was supported by the National Science Foundation (Grant MPS 75-03056) and the National Institute of General Medical Sciences, U.S. Public Health Service (Grants GM 22432, 10224, and 11072), to whom grateful acknowledgment is made. We wish to thank Dr. Craig Bradley of Bruker Scientific, Inc., and Ms. Valerie Hu for their assistance in measuring the ^{15}N and ^{1}H NMR spectra.

References and Notes

(1) Division of Chemistry and Chemical Engineering, California Institute of Technology, Pasadena, Calif. 91125.
(2) Alfred P. Sloan Fellow, 1976-1978.
(3) J. E. Bercaw, E. Rosenberg, and J. D. Roberts, *J. Am. Chem. Soc.*, **96**, 612 (1974).
(4) J. E. Bercaw, *J. Am. Chem. Soc.*, **96**, 5087 (1974).
(5) J. M. Manriquez and J. E. Bercaw, *J. Am. Chem. Soc.*, **96**, 6229 (1974).
(6) J. M. Manriquez, R. D. Sanner, R. E. Marsh, and J. E. Bercaw, *J. Am. Chem. Soc.*, **98**, 3042 (1976).
(7) R. D. Sanner, J. M. Manriquez, R. E. Marsh, and J. E. Bercaw, *J. Am. Chem. Soc.*, **98**, 8351 (1976).
(8) R. D. Sanner, D. M. Duggan, T. C. McKenzie, R. E. Marsh, and J. E. Bercaw, *J. Am. Chem. Soc.*, **98**, 8358 (1976).
(9) G. Binsch and D. A. Kleier, "The Computation of Complex Exchange Broadened NMR Spectra Computer Program DNMR", Quantum Chemistry Program Exchange, 1969.
(10) T. L. Brown, D. W. Dickerhoff, D. A. Bafus, and G. L. Morgan, *Rev. Sci. Instrum.*, **33**, 491 (1962).
(11) J. E. Bercaw, R. H. Marvich, L. G. Bell, and H. H. Brintzinger, *J. Am. Chem. Soc.*, **94**, 1219 (1972).
(12) Biorad "$^{15}N_2$": $^{15}N{\equiv}^{15}N$, 93.4%; $^{15}N{\equiv}^{14}N$, 6.3%; $^{14}N{\equiv}^{14}N$, 0.3%. $^{15}N^{14}N$: $^{15}N{\equiv}^{15}N$, 1.9%; $^{15}N{\equiv}^{14}N$, 89.6%; $^{14}N{\equiv}^{14}N$, 8.5%.
(13) Sample decomposition above 50 °C precluded measuring spectra at higher temperatures.
(14) F. Basolo and A. Wojcicki, *J. Am. Chem. Soc.*, **83**, 520 (1961).
(15) H. A. McKay, *Nature (London)*, **142**, 997 (1938).

Tetracarbon Metallocarboranes. 4.[1] Structure of the Nido System $(\eta^5\text{-}C_5H_5)Co(CH_3)_4C_4B_7H_6OC_2H_5$. The Problem of the Structural Diversity of Electronically Analogous Cage Systems

J. Robert Pipal and Russell N. Grimes*

Contribution from the Department of Chemistry, University of Virginia, Charlottesville, Virginia 22901. *Received October 11, 1977*

Abstract: The crystal structure of 12-(C_2H_5O)-1,2,3,7,8-$(\eta^5\text{-}C_5H_5)Co(CH_3)_4C_4B_7H_6$, a red, air-stable metallocarborane, has been determined from a single-crystal x-ray diffraction study. The molecule has a novel structure resembling a severely distorted icosahedron whose two halves have been partially separated, creating a huge opening on one side. The structure can be viewed as a derivative of $(CH_3)_4C_4B_8H_8$ in which an apex BH unit has been replaced by $(\eta^5\text{-}C_5H_5)Co$, and the central C-C bond in the cage has been severed. The title compound is the fifth example of a 12-vertex, 28-electron cage system to have been structurally characterized, the others being the $R_2C_2B_{10}H_{11}^-$ ion (R = C_6H_5 or CH_3), $(CH_3)_4C_4B_8H_8$, $(\eta^5\text{-}C_5H_5)Fe(CH_3)_4C_4B_7H_8$, and $(\eta^5\text{-}C_5H_5)_2Co_2C_4B_6H_{10}$. The fact that four distinctly different cage geometries are represented in this group of five compounds, despite their cage-isoelectronic relationship, is discussed in relation to the skeletal electron-count theory for cluster compounds, and some limitations of the theory are examined. Crystal data follow: space group $P2_1/n$; a = 8.322 (3), b = 14.284 (5), c = 16.810 (8) Å; β = 102.94 (3)°; ρ_{calcd} = 1.230 g cm^{-3} for Z = 4. The structure was refined by full-matrix least-squares methods to a final R value of 0.065 and R_w of 0.083 for the 1808 reflections for which $F_o^2 > 3\sigma(F_o^2)$.

The success of the polyhedral skeletal electron-count theory[2] in rationalizing the geometries of a wide array of cage and cluster compounds and in providing a reliable means of predicting the structures of new species is well documented.[2,3] The theory is particularly useful in dealing with cluster systems which are not readily amenable to detailed molecular orbital calculations, such as those having low symmetry or containing several types of framework atoms. While full awareness of these ideas among chemists has not yet arrived, inorganic textbooks have begun to incorporate them, and in time the art of skeletal electron counting may be as familiar in chemical education as is, for example, the valence shell electron pair repulsion (VSEPR) model.[4]

Like the VSEPR and other qualitative approaches to chemical bonding, it is inevitable that limits to the utility of the skeletal electron-count theory will be found; situations will be discovered in which the theory can be applied only with modification, and others in which it fails altogether. It is obviously important to the further development of cluster chemistry to probe these limiting cases and to try to identify the factors which cause deviation from the predicted structures. It can be hoped that in time this will lead to a more sophisticated version of the theory which will increase its usefulness still further.

In our work we have encountered several situations in which the electron-counting rules are violated, a recent example being the 14-vertex $(\eta^5\text{-}C_5H_5)_2Fe_2(CH_3)_4C_4B_8H_8$ isomers which are discussed elsewhere.[5] In the present article we describe the crystallographic structure determination of a recently prepared[6] metallocarborane, $(\eta^5\text{-}C_5H_5)Co(CH_3)_4C_4B_7H_6OC_2H_5$, which is one of five structurally established examples of a 12-vertex, 28-electron cage system. Of these five compounds, we are amazed to find that no fewer than four markedly different polyhedral geometries are represented, and hence a detailed comparison of their structures seems warranted.

Experimental Section

Red crystals of 12-(C_5H_5O)-1,2,3,7,8-$(\eta^5\text{-}C_5H_5)Co(CH_3)_4C_4B_7H_6$, prepared[6] by the treatment of $[(CH_3)_2C_2B_4H_4]_2FeH_2$ with $CoCl_2$ and C_5H_6 in ethanolic KOH at 70 °C, were grown by the vapor diffusion of pentane into a methylene chloride solution of the compound. One crystal was mounted on a glass fiber in an arbitrary orientation and examined by preliminary precession photographs which indicated acceptable crystal quality. The chosen crystal was a rectangular parallelepiped with one edge truncated, creating a seventh face. Approximate maximum dimensions were 0.21 × 0.23 × 0.48 mm. Crystal data follow: $CoOC_{15}B_7H_{28}$; mol wt 359.00; space group

0002-7863/78/1500-3083$01.00/0